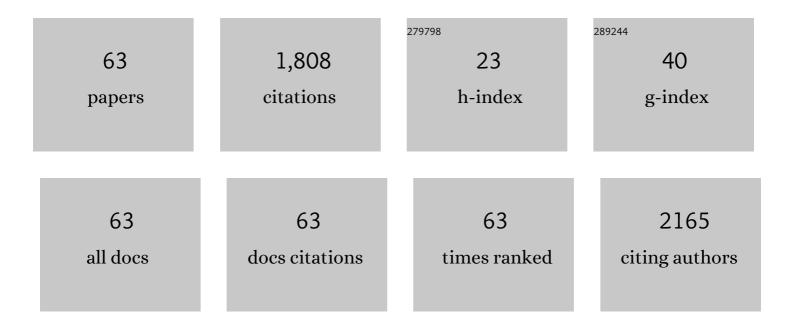
Liyun Cao

List of Publications by Year in descending order

Source: https://exaly.com/author-pdf/8401077/publications.pdf Version: 2024-02-01



#	Article	IF	CITATIONS
1	High stability SEI film on the surface of Sb2O5/carbon cloth by coating SiO2 as high performance LIBs and SIBs anodes. Journal of Alloys and Compounds, 2022, 891, 162031.	5.5	10
2	A three-dimensional coral-like Zn,O-codoped Ni3S2 electrocatalyst for efficient overall water splitting at a large current density. Sustainable Energy and Fuels, 2022, 6, 466-473.	4.9	0
3	Molybdenum and cobalt co-doped VC nanoparticles encapsulated in nanocarbon as efficient electrocatalysts for the hydrogen evolution reaction. Inorganic Chemistry Frontiers, 2022, 9, 870-878.	6.0	13
4	Dual modulation of morphology and electronic structures of VN@C electrocatalyst by W doping for boosting hydrogen evolution reaction. Chinese Chemical Letters, 2022, 33, 4781-4785.	9.0	17
5	Dual carbon composited with Co9S8 through C-S bond as a high performance Binder-Free anode for Sodium-Ion batteries. Applied Surface Science, 2022, 582, 152406.	6.1	9
6	<i>In situ</i> construction of superhydrophilic crystalline Ni ₃ S ₂ @amorphous VO _{<i>x</i>} heterostructure nanorod arrays for the hydrogen evolution reaction with industry-compatible current density. Dalton Transactions, 2022, 51, 7234-7240.	3.3	5
7	Ultrafine VN nanoparticles confined in Co@N-doped carbon nanotubes for boosted hydrogen evolution reaction. Journal of Alloys and Compounds, 2021, 853, 157257.	5.5	22
8	A thick titanium dioxide layer formed by Co-doping on a carbon surface promotes the polysulfide-adsorption ability in Li–S batteries. Sustainable Energy and Fuels, 2021, 5, 4153-4160.	4.9	1
9	Tuning the morphologic and electronic structures of self-assembled NiSe/Ni3Se2 heterostructures with vanadium doping toward efficient electrocatalytic hydrogen production. Applied Surface Science, 2021, 542, 148598.	6.1	20
10	Realizing Fast Charge Diffusion in Oriented Iron Carbodiimide Structure for High-Rate Sodium-Ion Storage Performance. ACS Nano, 2021, 15, 6410-6419.	14.6	41
11	Vanadium-doped hierarchical Cu2S nanowall arrays assembled by nanowires on copper foam as an efficient electrocatalyst for hydrogen evolution reaction. Scripta Materialia, 2021, 196, 113756.	5.2	16
12	Exposing WS2 nanosheets edge by supports carbon structure: Guiding Na+ intercalation along (0 0 2) plane for enhanced reaction kinetics and stability. Chemical Engineering Journal, 2021, 411, 128554.	12.7	17
13	Rational Design of Vanadium-Modulated Ni ₃ Se ₂ Nanorod@Nanosheet Arrays as a Bifunctional Electrocatalyst for Overall Water Splitting. ACS Sustainable Chemistry and Engineering, 2021, 9, 12005-12016.	6.7	38
14	Guiding Fabrication of Continuous Carbon-Confined Sb ₂ Se ₃ Nanoparticle Structure for Durable Potassium-Storage Performance. ACS Applied Energy Materials, 2021, 4, 10391-10403.	5.1	10
15	Intrinsic defects promote rapid conversion of polysulfides on carbon surface to achieve high rate performance. Carbon, 2021, 183, 899-911.	10.3	10
16	Binding Molybdenum selenide with dual conductive carbon as Self-Supporting anode for an efficient sodium storage. Applied Surface Science, 2021, 570, 151122.	6.1	1
17	Vanadium -mediated ultrafine Co/Co ₉ S ₈ nanoparticles anchored on Co–N-doped porous carbon enable efficient hydrogen evolution and oxygen reduction reactions. Nanoscale, 2021, 13, 16277-16287.	5.6	11
18	Inducing [100]-orientated plate-like α-MoO3 to achieve regularly exfoliated layer structure enhancing Li storage performance. Journal of Materials Science: Materials in Electronics, 2021, 32, 3006-3018.	2.2	5

LIYUN CAO

#	Article	IF	CITATIONS
19	Self-templated induced carbon-supported hollow WS ₂ composite structure for high-performance sodium storage. Journal of Materials Chemistry A, 2021, 9, 21366-21378.	10.3	8
20	Controlled Synthesis of V-Doped Heterogeneous Ni ₃ S ₂ /NiS Nanorod Arrays as Efficient Hydrogen Evolution Electrocatalysts. Langmuir, 2021, 37, 357-365.	3.5	10
21	Heterostructured VN/Mo ₂ C Nanoparticles as Highly Efficient pH-Universal Electrocatalysts toward the Hydrogen Evolution Reaction. ACS Sustainable Chemistry and Engineering, 2021, 9, 15202-15211.	6.7	22
22	Fe ₂ P encapsulated in carbon nanowalls decorated with well-dispersed Fe ₃ C nanodots for efficient hydrogen evolution and oxygen reduction reactions. Nanoscale, 2021, 13, 17920-17928.	5.6	10
23	Methanol-assisted synthesis of Ni ³⁺ -doped ultrathin NiZn-LDH nanomeshes for boosted alkaline water splitting. Dalton Transactions, 2020, 49, 1325-1333.	3.3	27
24	Carbon capsule confined Sb ₂ Se ₃ for fast Na ⁺ extraction in sodium-ion batteries. Sustainable Energy and Fuels, 2020, 4, 797-808.	4.9	12
25	Cu/Cu2O@Ppy nanowires as a long-life and high-capacity anode for lithium ion battery. Chemical Engineering Journal, 2020, 391, 123597.	12.7	50
26	Controllable Conversion from Single-Crystal Nanorods to Polycrystalline Nanosheets of NiCoV-LTH for Oxygen Evolution Reaction at Large Current Density. ACS Sustainable Chemistry and Engineering, 2020, 8, 16091-16096.	6.7	25
27	Mo-Doped ultrafine VC nanoparticles confined in few-layer graphitic nanocarbon for improved electrocatalytic hydrogen evolution. Inorganic Chemistry Frontiers, 2020, 7, 4142-4149.	6.0	10
28	Controlled WS2 crystallinity effectively dominating sodium storage performance. Journal of Energy Chemistry, 2020, 51, 143-153.	12.9	17
29	Layered-structure (NH ₄) ₂ Mo ₄ O ₁₃ @N-doped porous carbon composite as a superior anode for lithium-ion batteries. Chemical Communications, 2020, 56, 7757-7760.	4.1	7
30	In Situ Construction of "Anchorâ€Like―Structures in FeNCN for Long Cyclic Life in Sodiumâ€Ion Batteries. Advanced Functional Materials, 2020, 30, 2000208.	14.9	19
31	In-situ optimizing the valence configuration of vanadium sites in NiV-LDH nanosheet arrays for enhanced hydrogen evolution reaction. Journal of Energy Chemistry, 2020, 47, 263-271.	12.9	66
32	Co–N-doped single-crystal V3S4 nanoparticles as pH-universal electrocatalysts for enhanced hydrogen evolution reaction. Electrochimica Acta, 2020, 335, 135696.	5.2	11
33	Polyethylene glycol (PEG)-assisted synthesis of self-assembled cactus-like NH4V3O8 for lithium ion battery cathode. Scripta Materialia, 2020, 183, 75-80.	5.2	4
34	V-Doping Triggered Formation and Structural Evolution of Dendritic Ni ₃ S ₂ @NiO Core–Shell Nanoarrays for Accelerating Alkaline Water Splitting. ACS Sustainable Chemistry and Engineering, 2020, 8, 6222-6233.	6.7	66
35	Nanoporous NiAl-LDH nanosheet arrays with optimized Ni active sites for efficient electrocatalytic alkaline water splitting. Sustainable Energy and Fuels, 2020, 4, 2850-2858.	4.9	56
36	Rice crust-like Fe3O4@C/rGO with improved extrinsic pseudocapacitance for high-rate and long-life Li-ion anodes. Journal of Alloys and Compounds, 2019, 804, 57-64.	5.5	27

Liyun Cao

#	Article	IF	CITATIONS
37	Formation of hierarchical Ni3S2 nanohorn arrays driven by in-situ generation of VS4 nanocrystals for boosting alkaline water splitting. Applied Catalysis B: Environmental, 2019, 257, 117911.	20.2	92
38	Design of an ultra-stable Sb2Se3 anode with excellent Na storage performance. Journal of Alloys and Compounds, 2019, 810, 151930.	5.5	8
39	Controlling the thickness of amorphous layer on Cu3(PO4)2 particle for promoted sodium storage reversibility as a conversion-reaction-based cathode. Journal of Electroanalytical Chemistry, 2019, 852, 113406.	3.8	4
40	Synthesis, characterization and photocatalytic properties of nanoscale pyrochlore type Bi2Zr2O7. Materials Science and Engineering B: Solid-State Materials for Advanced Technology, 2019, 240, 133-139.	3.5	12
41	N-doped TiO2/rGO hybrids as superior Li-ion battery anodes with enhanced Li-ions storage capacity. Journal of Alloys and Compounds, 2019, 784, 165-172.	5.5	27
42	Co,N-Codoped porous vanadium nitride nanoplates as superior bifunctional electrocatalysts for hydrogen evolution and oxygen reduction reactions. Nanoscale, 2019, 11, 11542-11549.	5.6	53
43	SnSe/r-GO Composite with Enhanced Pseudocapacitance as a High-Performance Anode for Li-Ion Batteries. ACS Sustainable Chemistry and Engineering, 2019, 7, 8637-8646.	6.7	55
44	Tuning the coupling interface of ultrathin Ni ₃ S ₂ @NiV-LDH heterogeneous nanosheet electrocatalysts for improved overall water splitting. Nanoscale, 2019, 11, 8855-8863.	5.6	133
45	Improved Li-Storage Properties of Cu ₂ V ₂ O ₇ Microflower by Constructing an in Situ CuO Coating. ACS Sustainable Chemistry and Engineering, 2019, 7, 6267-6274.	6.7	20
46	Sulfur-regulated the binding configurations of nitrogen in three-dimensional graphene to improve lithium storage kinetics. Journal of Alloys and Compounds, 2019, 786, 1013-1020.	5.5	16
47	A N/S-codoped disordered carbon with enlarged interlayer distance derived from cirsium setosum as high-performance anode for sodium ion batteries. Journal of Materials Science: Materials in Electronics, 2019, 30, 21323-21331.	2.2	2
48	Design of Cu2O coated Cu3V2O7(OH)2·2H2O microflower with in-situ crystallization process and enhanced Li-storage properties. Journal of Electroanalytical Chemistry, 2019, 835, 186-191.	3.8	9
49	A new approach to preparing Bi ₂ Zr ₂ O ₇ photocatalysts for dye degradation. Materials Research Express, 2018, 5, 015039.	1.6	8
50	Design of dual-carbon modified MnO electrode improves adsorption and conversion reaction in Li-ion batteries. Ceramics International, 2018, 44, 3248-3254.	4.8	14
51	3D self-assembled VS ₄ microspheres with high pseudocapacitance as highly efficient anodes for Na-ion batteries. Nanoscale, 2018, 10, 21671-21680.	5.6	47
52	Well-dispersed ultrasmall VC nanoparticles embedded in N-doped carbon nanotubes as highly efficient electrocatalysts for hydrogen evolution reaction. Nanoscale, 2018, 10, 14272-14279.	5.6	58
53	In situ synthesis of mesoporous C-doped TiO 2 single crystal with oxygen vacancy and its enhanced sunlight photocatalytic properties. Dyes and Pigments, 2017, 144, 203-211.	3.7	55
54	Adjusting the Chemical Bonding of SnO ₂ @CNT Composite for Enhanced Conversion Reaction Kinetics. Small, 2017, 13, 1700656.	10.0	111

LIYUN CAO

#	Article	IF	CITATIONS
55	Enhanced cyclic performance of Cu2V2O7/ reduced Graphene Oxide mesoporous microspheres assembled by nanoparticles as anode for Li-ion battery. Journal of Alloys and Compounds, 2017, 724, 421-426.	5.5	25
56	Controlling the Sn–C bonds content in SnO ₂ @CNTs composite to form <i>in situ</i> pulverized structure for enhanced electrochemical kinetics. Nanoscale, 2017, 9, 18681-18689.	5.6	56
57	Rape seed shuck derived-lamellar hard carbon as anodes for sodium-ion batteries. Journal of Alloys and Compounds, 2017, 695, 632-637.	5.5	71
58	Facile synthesis of reduced graphene oxide/NH ₄ V ₃ O ₈ with high capacity as a cathode material for lithium ion batteries. Micro and Nano Letters, 2017, 12, 940-943.	1.3	5
59	Controlling the layered structure of WS2 nanosheets to promote Na+ insertion with enhanced Na-ion storage performance. Electrochimica Acta, 2016, 222, 1724-1732.	5.2	28
60	High Pseudocapacitance in FeOOH/rGO Composites with Superior Performance for High Rate Anode in Li-Ion Battery. ACS Applied Materials & Interfaces, 2016, 8, 35253-35263.	8.0	119
61	Structure-controlled synthesis and electrochemical properties of NH4V3O8 as cathode material for Lithium ion batteries. Electrochimica Acta, 2016, 212, 217-224.	5.2	20
62	Improved Na Storage Performance with the Involvement of Nitrogen-Doped Conductive Carbon into WS ₂ Nanosheets. ACS Applied Materials & Interfaces, 2016, 8, 23899-23908.	8.0	65
63	Equal contents of intrinsic defects and oxygen-containing defects promote carbon electrodes to achieve high sulfur loads. Journal of Nanostructure in Chemistry, 0, , 1.	9.1	2